

Electron Diffraction

Anargha Mondal^{*1}

¹IISER Pune

August 20, 2025

Abstract

This report outlines an experiment to demonstrate the wave nature of electrons through diffraction by a polycrystalline graphite target. Electrons are accelerated by a high voltage potential, and their subsequent diffraction pattern is observed on a fluorescent screen. By measuring the diameters of the diffraction rings at various accelerating voltages, the de Broglie wavelength of the electrons can be determined using the Bragg condition. Finally, we plot the theoretical (de Broglie) wavelength against the experimentally obtained (Bragg) wavelength to ensure that indeed, they measure the same quantity and electrons indeed behave as waves as well as particles.

1 Introduction

In 1924, Louis de Broglie revolutionized modern physics by postulating that all matter exhibits wave-like properties. This hypothesis extended the concept of wave-particle duality, previously attributed only to light, to particles such as electrons. De Broglie proposed that a particle with momentum p has an associated wavelength λ given by the equation $\lambda = h/p$, where h is Planck's constant. This groundbreaking idea was experimentally confirmed in 1927 by Clinton Davisson and Lester Germer, who observed the diffraction of electrons from a single crystal of nickel.

The electron diffraction experiment provides a compelling demonstration of the wave nature of electrons. By accelerating electrons through a known potential difference, they gain a predictable momentum and, consequently, a specific de Broglie wavelength. When these electrons pass through a crystalline structure, such as the atomic lattice of graphite, they diffract in a manner analogous to X-rays, producing a characteristic interference pattern of concentric rings. The analysis of this pattern allows for the direct calculation of the electron's wavelength, offering a method to verify de Broglie's foundational hypothesis and explore a cornerstone of quantum mechanics.

In this experiment, a beam of electrons is accelerated and directed onto a thin polycrystalline graphite foil. Due to the ordered atomic planes, the electrons undergo Bragg diffraction, forming concentric rings on a fluorescent screen. Measuring the radii of these rings at different accelerating voltages allows one to confirm the de Broglie wavelength and thereby establish the dual nature of matter.

2 Theory

The theoretical basis of this experiment combines de Broglie's hypothesis with the principles of Bragg diffraction.

2.1 De Broglie Wavelength

According to de Broglie, the wavelength (λ) of a particle is inversely proportional to its momentum (p):

$$\lambda = \frac{h}{p} \tag{1}$$

^{*}20221042

where h is Planck's constant (6.626×10^{-34} J·s).

For an electron of mass m and charge e accelerated from rest through a potential difference V , its kinetic energy (KE) is given by:

$$KE = eV \quad (2)$$

Assuming non-relativistic speeds, the kinetic energy can also be expressed as:

$$KE = \frac{p^2}{2m} \quad (3)$$

By equating these two expressions for kinetic energy, we can solve for the momentum:

$$p = \sqrt{2meV} \quad (4)$$

Substituting this into the de Broglie relation gives the theoretical wavelength of the electron as a function of the accelerating voltage:

$$\lambda = \frac{h}{\sqrt{2meV}} \quad (5)$$

2.2 Bragg Diffraction

When the electron waves interact with the polycrystalline graphite target, they are diffracted by the planes of carbon atoms in the crystal lattice. A polycrystalline target consists of many microscopic crystals (crystallites) oriented randomly. Due to this random orientation, some crystallites will always be positioned at the correct angle to satisfy the Bragg condition for constructive interference.

Bragg's law describes the condition for constructive interference from a crystal lattice:

$$n\lambda = 2d \sin \theta \quad (6)$$

where n is an integer (the order of diffraction, typically $n=1$ for this experiment), λ is the wavelength of the incident wave, d is the spacing between the atomic planes in the crystal, and θ is the glancing angle (the angle between the incident beam and the crystal plane).

For graphite, there are two primary interplanar spacings that produce observable diffraction rings:

- $d_{10} = 213$ pm (2.13×10^{-10} m)
- $d_{11} = 123$ pm (1.23×10^{-10} m)

In the experimental setup, the diffracted electrons travel a distance L from the graphite target to the fluorescent screen, where they form concentric rings of diameter D . The relationship between the ring diameter, the distance L , and the diffraction angle 2θ can be approximated for small angles as:

$$\tan(2\theta) \approx \frac{D}{2L}$$

Since the angles are very small, we can use the approximation $\sin \theta \approx \tan \theta \approx \theta$. Therefore, the Bragg angle θ can be related to the ring geometry. A more precise geometric analysis gives:

$$\sin(2\theta) = \frac{D}{2R_{\text{tube}}} \quad (7)$$

where R_{tube} is the radius of curvature of the spherical screen. Combining this with Bragg's law allows for the experimental determination of the electron's wavelength.

It is worthwhile to be noted that electron diffraction done in the setup provided is an example of a *Fraunhofer* (far-field) approach. In the development of the formalism we only assume kinematical diffraction, i.e., the electrons are scattered only once off of the lattice.

2.3 Core elements of electron diffraction: A Quantum Mechanical treatment

We lay out a purely quantum mechanical calculation for obtaining the diffraction pattern:

The electrons are considered as plane waves, and is a superposition of states like $|\psi\rangle = \exp(2\pi i \mathbf{k} \cdot \mathbf{r})$. Note that a fully relativistic treatment (since the electrons move at an appreciable fraction of the speed of light in vacuum) warrants the use of the Dirac equation, but since spin is generally unimportant, we can reduce it to the Klein-Gordon equation. However, following Fujiwara [1], a lot of the complications can be side-stepped as follows. The relationship between the total energy of the electrons and the wavevector is written as:

$$E = \frac{\hbar^2 k^2}{2m^*}$$

with

$$m^* = m_0 + \frac{E}{2c^2}$$

where \hbar is the Planck constant, m^* is a relativistic effective mass used to cancel out the relativistic terms for electrons of energy and m_0 the rest mass of the electron. The concept of effective mass occurs throughout physics. (see for instance [2] and comes up in the behavior of quasiparticles.

The wavelength of the electrons λ in vacuum is from the above equations

$$\lambda = \frac{2\pi}{k} = \frac{\hbar}{\sqrt{2m^* E}} = \frac{\hbar c}{\sqrt{E(2m_0 c^2) + E}}$$

The high-energy electrons interact with the Coulomb potential,[33] which for a crystal can be considered in terms of a Fourier series:

$$V(r) = \sum_g V_g \exp(2\pi i g \cdot r)$$

Around each reciprocal lattice point one has this shape function, which is the Fourier transform of the geometry of the crystal. How much intensity there will be in the diffraction pattern depends upon the intersection of the Ewald sphere, that is energy conservation, and the shape function around each reciprocal lattice.

The result is that the electron wave after it has been diffracted can be written as an integral over different plane waves:

$$\psi(r) = \int \phi(k) \exp(2\pi i \mathbf{k} \cdot \mathbf{r}) d^3 \mathbf{k}$$

The integral is over the k s that satisfy the Ewald condition. We also have $I(k) = |\phi(k)|^2$ Diffraction patterns depend on whether the beam is diffracted by one single crystal or by a number of differently oriented crystallites, for instance in a polycrystalline material. If there are many contributing crystallites, or different lattice constants in different directions, the diffraction image is a superposition of individual crystal patterns (in Fourier space). With a large number of grains this superposition yields diffraction spots of all possible reciprocal lattice vectors. This is the exact observation we see for graphite, as will be shown. We work under the kinematic assumption, and hence we write, for each diffraction point \mathbf{g} :

$$I_g = |\phi(k)|^2 \propto \left| F_g \frac{\sin(\pi t s_z)}{\pi s_z} \right|^2$$

Here, F_g is the structure factor:

$$F_g = \sum_{j=1}^N f_j \exp(2\pi i \mathbf{g} \cdot \mathbf{r}_j - T_j g^2)$$

and the Laue condition is satisfied:

$$k = k_0 + g + s_z$$

2.4 Ring diffraction pattern in Graphite

We use the reflection sphere construction [3]. In the reciprocal space, we write the amplitude as:

$$\phi_g = \sum_n F_n \exp(-2\pi i \mathbf{K}' \cdot \mathbf{r}_n) \quad (8)$$

$$= \sum_n F_n \exp(-2\pi i(n_1 \zeta_1 + n_2 \zeta_2 + n_3 \zeta_3)) \quad (9)$$

where n_i s are the coordinates in real space and ζ_i s are the coordinates in reciprocal space. For a strong, single reflection, we can impose the Lau condition as follows:

$$\mathbf{g} = \mathbf{k}' - \mathbf{k} \quad (10)$$

Hence, we can construct a *Ewald sphere*-like construction, called the *reflection sphere*. Wherever the sphere intersects a reciprocal lattice point produces a strong (Bragg) reflection. The radii of the diffraction ring, for small angles, after using the Bragg diffraction condition $R = \frac{\lambda L}{d}$ is hence given by:

$$R_{hkl} = \frac{\lambda L}{d_{hkl}} = \frac{\lambda L}{a} \sqrt{(h^2 + k^2 + l^2)} \quad (11)$$

All other diffraction rings occur as integer multiples of this (principal) radius. The graphite crystal, has two crystal structures, with the corresponding Miller indices:

$$100, 110$$

with corresponding $d = 0.213\text{nm}$ and 0.123 nm , respectively. Plugging in the suitable values of hkl , we get

$$R_{100} = \frac{\lambda L}{a_{100}} \quad (12)$$

$$R_{110} = \frac{\lambda L \sqrt{2}}{a_{110}} \quad (13)$$

3 Experimental Apparatus

The experiment is conducted using an electron diffraction tube, which is a highly evacuated glass bulb containing the following key components:

1. **Electron Gun:** This assembly generates and accelerates the electrons.
 - **Filament:** A heated filament releases electrons through thermionic emission.
 - **Cathode:** Serves as the source of the emitted electrons.
 - **Anode:** A high positive potential is applied to the anode to accelerate the electrons towards the target, forming a focused beam.
2. **Graphite Target:** A thin foil of polycrystalline graphite is placed in the path of the electron beam. The carbon atoms in the graphite's hexagonal lattice structure act as a natural diffraction grating.
3. **Fluorescent Screen:** The inner surface of the glass bulb is coated with a fluorescent material. When the diffracted electrons strike this screen, it emits light, making the concentric diffraction rings visible.

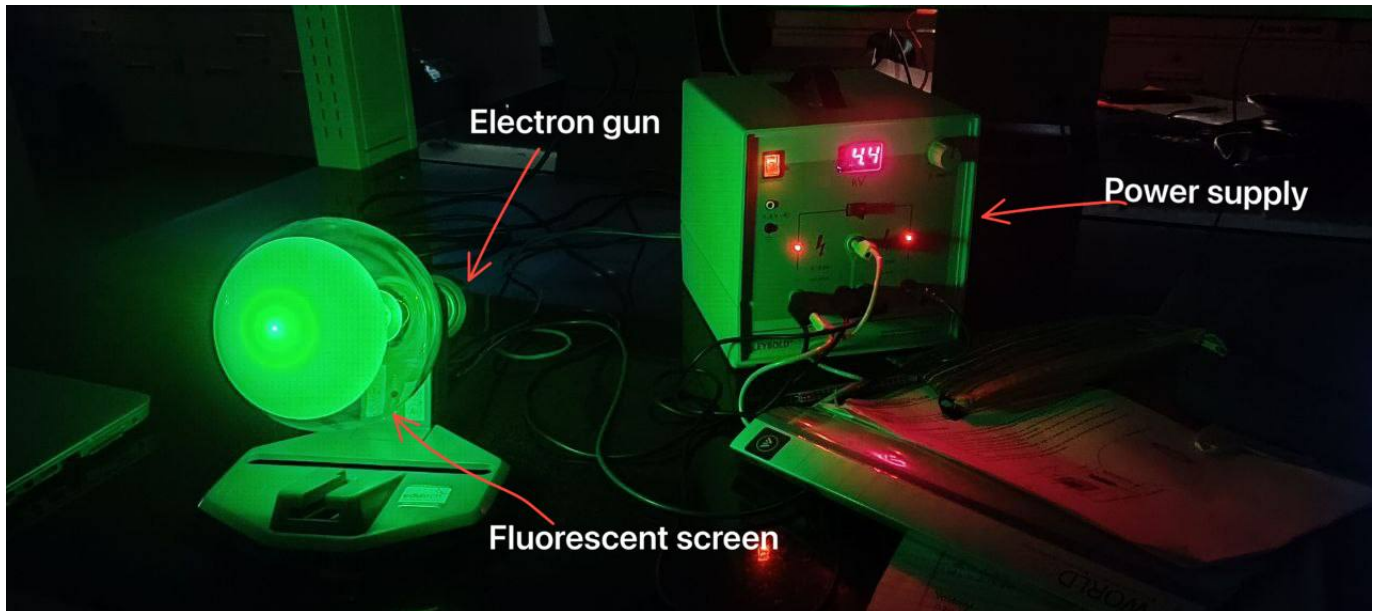


Figure 1: Apparatus

4. **High Voltage Power Supply:** A power supply capable of providing several kilovolts (e.g., 2-5 kV) is required to accelerate the electrons to a high enough momentum to have a wavelength suitable for diffraction by the graphite lattice.
5. **Heater Supply:** A low-voltage power supply is needed to heat the filament of the electron gun.
6. **Calipers or Ruler:** A measuring instrument is used to determine the diameter of the visible diffraction rings on the screen.

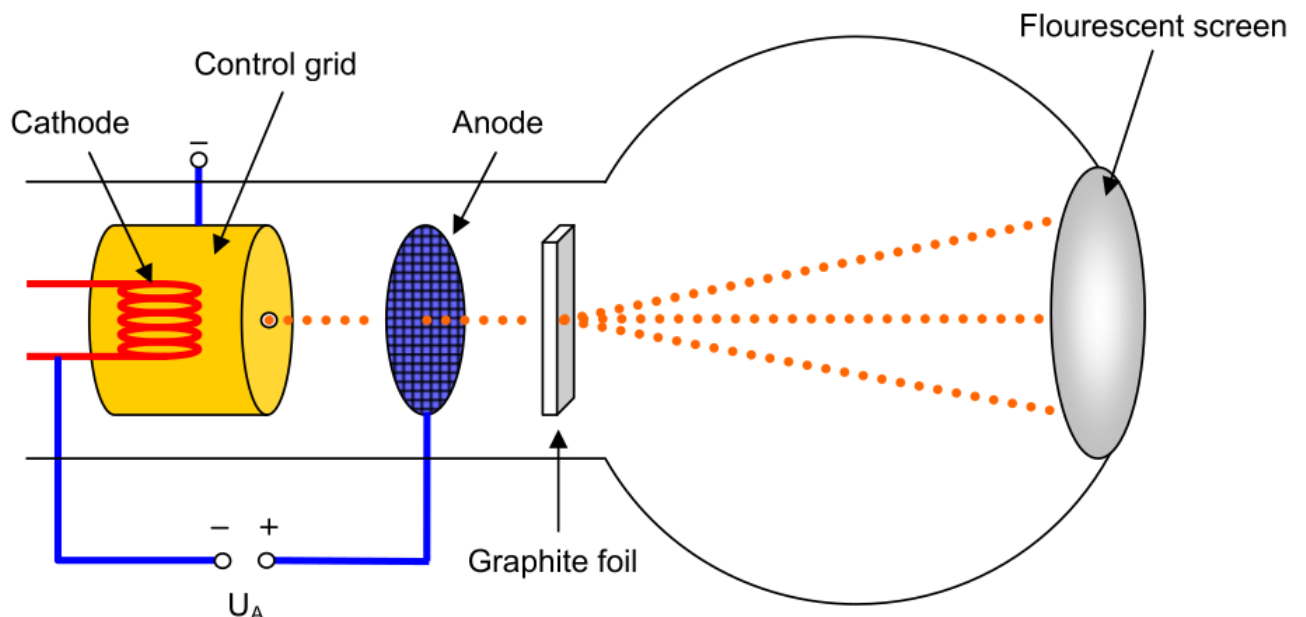


Figure 2: Electron Gun

4 Data Collection

The experiment requires systematic collection of diffraction ring diameters at varying accelerating voltages. The following procedure was followed:

1. The accelerating voltage was varied in steps of 500 V over the range 2.5–5.0 kV. At each step, the beam was refocused for maximum clarity of diffraction rings.
2. For each voltage, the diameters of both the inner and outer diffraction rings were measured directly on the fluorescent screen using vernier calipers.
3. To reduce random error, three independent measurements of each ring diameter were taken and averaged.
4. The averaged diameters were recorded along with the corresponding accelerating voltage in a data table for later analysis.

This dataset was then used to calculate the diffraction angles and corresponding wavelengths for comparison with theoretical de Broglie predictions.

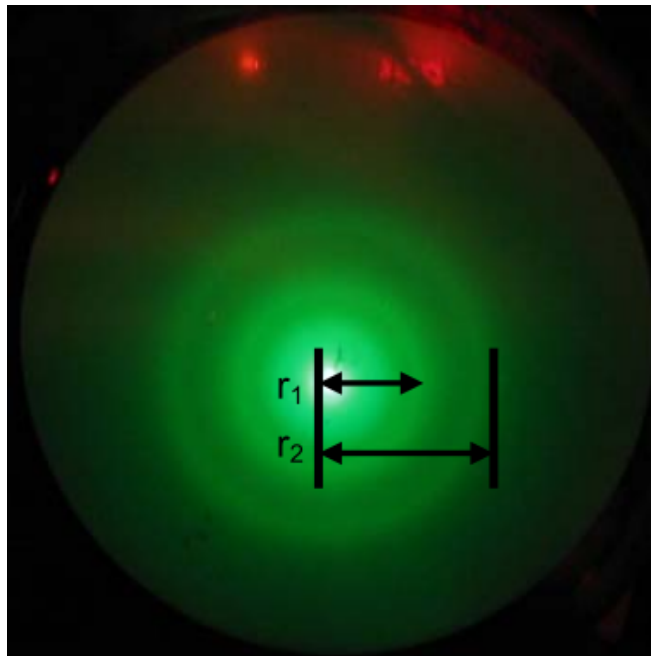


Figure 3: Correct measurements

5 Results

First of all, we must account for the curvature of the fluorescent screen. Hence we write, from geometry and $\sin\theta_i = \tan\theta_i$:

$$\sin\theta_i = \frac{D \sin(\frac{d_i}{2D})}{2L}$$

where $L = 127\text{mm}$ is the length of the tube, $D = 130\text{mm}$ is the diameter of the flask. Plugging this in the Bragg equation, the principal ring is given by:

$$2d_{100}\sin\left(\frac{D \sin(\frac{d_i}{2D})}{2L}\right) = \lambda_{100} \quad (14)$$

$$2d_{110}\sin\left(\frac{D \sin(\frac{d_i}{2D})}{2L}\right) = \lambda_{110} \quad (15)$$

V (kV)	D2 (mm)	$\sin \theta_2$	D1 (mm)	$\sin \theta_1$	λ_{100} [m]	λ_{110} [m]	$\lambda_{\text{de Broglie}}$ [m]
2.000e+00	3.140e+01	6.166e-02	5.462e+01	1.067e-01	2.627e-11	2.626e-11	2.746e-11
2.500e+00	2.888e+01	5.673e-02	4.948e+01	9.681e-02	2.417e-11	2.382e-11	2.456e-11
3.000e+00	2.660e+01	5.227e-02	4.500e+01	8.814e-02	2.227e-11	2.168e-11	2.242e-11
3.500e+00	2.462e+01	4.839e-02	4.240e+01	8.310e-02	2.062e-11	2.044e-11	2.075e-11
4.000e+00	2.280e+01	4.482e-02	4.002e+01	7.847e-02	1.910e-11	1.930e-11	1.941e-11
4.500e+00	2.168e+01	4.263e-02	3.722e+01	7.302e-02	1.816e-11	1.796e-11	1.830e-11
5.000e+00	2.060e+01	4.051e-02	3.528e+01	6.924e-02	1.726e-11	1.703e-11	1.736e-11

Table 1: Measured diffraction ring diameters, calculated Bragg wavelengths, and theoretical de Broglie wavelengths.

Theoretically, we expect all the wavelengths to be the same. Plotting, we get:

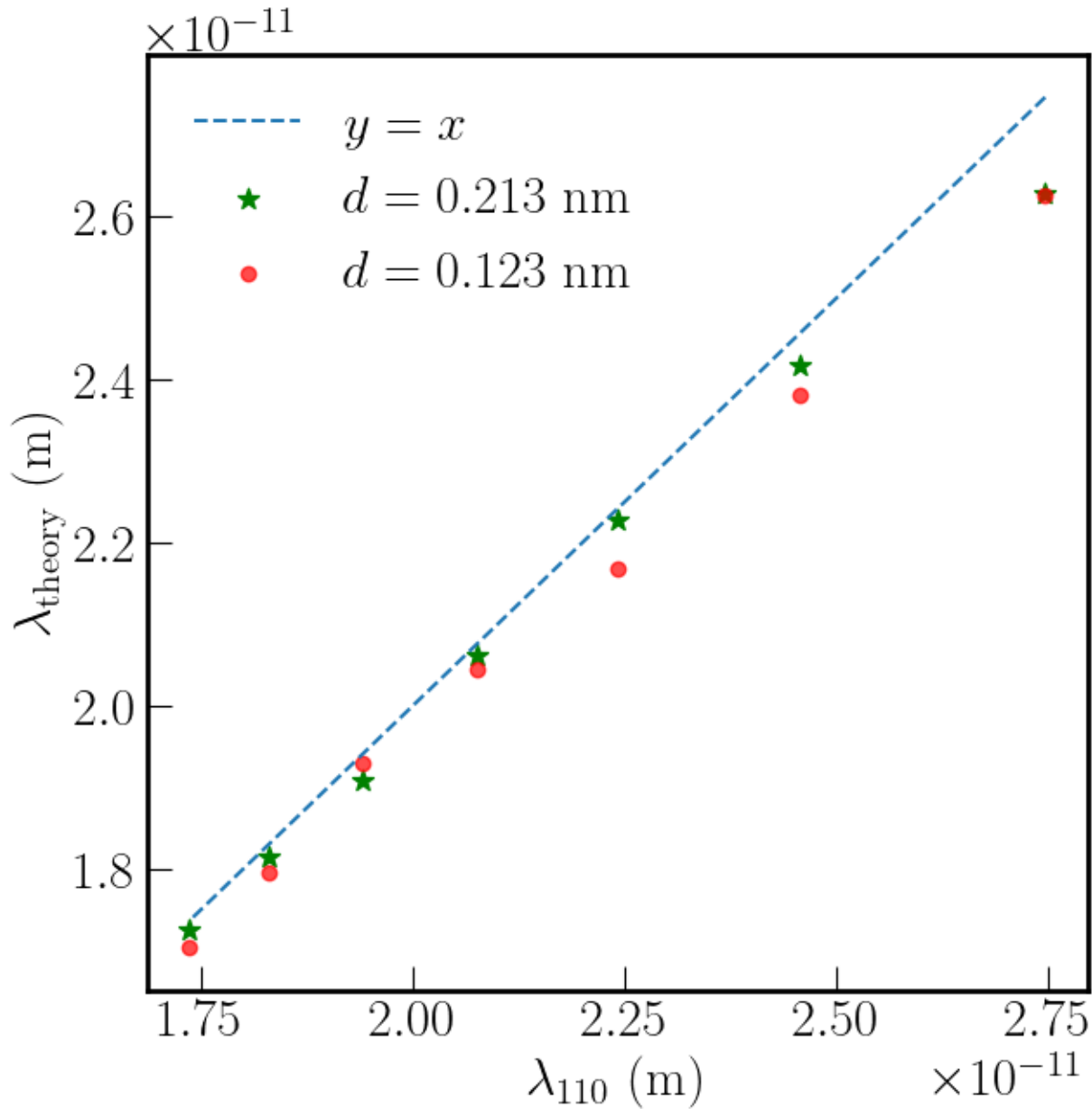


Figure 4: The theoretical expectations and our data points

6 Error Analysis

We use the `uncertainties` Python package to do our error propagation. First, we outline the error propagation:

Assumptions and primary error sources

The dominant experimental uncertainty arises from measuring the diffraction ring diameters D on the curved fluorescent screen with vernier calipers. We denote the diameter measurement uncertainty by ΔD . The distance from the graphite foil to the screen, L , also has a finite uncertainty ΔL (the manuals quote a typical ΔL of the order of a few mm); the lattice spacings d are taken from the literature and assumed to have negligible uncertainty for the purposes of the present student experiment. The accelerating voltage V has an uncertainty ΔV due to the power supply reading tolerance and stability.

Below we propagate these uncertainties to obtain the 1σ uncertainty in the experimentally determined wavelength λ (from Bragg) and the theoretical de Broglie wavelength λ_{th} .

Wavelength from Bragg's law and its uncertainty

From Bragg's law (first order, $n = 1$):

$$\lambda = 2d \sin \theta. \quad (1)$$

Using the approximation (A) we have

$$\lambda(D, L) \approx 2d \left(\frac{D}{2L} \right) = d \frac{D}{L}. \quad (2)$$

Thus, λ is, in this approximation, directly proportional to D and inversely proportional to L .

To propagate uncertainties we use standard first-order error propagation. If λ depends on variables x_i with uncertainties Δx_i that are uncorrelated, the variance of λ is

$$\sigma_{\lambda}^2 = \sum_i \left(\frac{\partial \lambda}{\partial x_i} \Delta x_i \right)^2. \quad (3)$$

Applying (3) to (2) for the variables D and L ,

$$\frac{\partial \lambda}{\partial D} = \frac{d}{L}, \quad \frac{\partial \lambda}{\partial L} = -d \frac{D}{L^2} = -\frac{\lambda}{L}.$$

Hence the combined 1σ uncertainty in λ is

$$\sigma_{\lambda} = \sqrt{\left(\frac{d}{L} \Delta D \right)^2 + \left(\frac{\lambda}{L} \Delta L \right)^2}. \quad (4)$$

By substituting $\lambda = dD/L$ the first term can also be written as $\lambda(\Delta D/D)$ and the second term as $\lambda(\Delta L/L)$, giving the intuitive approximate form

$$\sigma_{\lambda} \approx \lambda \sqrt{\left(\frac{\Delta D}{D} \right)^2 + \left(\frac{\Delta L}{L} \right)^2}. \quad (5)$$

Equation (5) is useful for quick estimates when $\Delta D \ll D$ and $\Delta L \ll L$.

Note on exact geometry: If the exact expression $\sin \theta = s(D, L, R)$ (including the screen curvature R) is used, then compute

$$\frac{\partial \lambda}{\partial D} = 2d \cos \theta \frac{\partial \theta}{\partial D} \quad \text{with} \quad \frac{\partial \theta}{\partial D} = \frac{1}{\sqrt{1-s^2}} \frac{\partial s}{\partial D},$$

and include the ΔR term if the uncertainty of R is relevant. The algebra is identical in spirit to the derivation above but uses the correct geometric function $s(D, L, R)$.

Uncertainty in theoretical de Broglie wavelength

The theoretical de Broglie wavelength of an electron accelerated through potential V is

$$\lambda_{\text{th}}(V) = \frac{h}{\sqrt{2m_e e V}}. \quad (6)$$

Differentiate (6) with respect to V to obtain the sensitivity:

$$\frac{\partial \lambda_{\text{th}}}{\partial V} = -\frac{1}{2} \frac{h}{\sqrt{2m_e e}} V^{-3/2} = -\frac{1}{2} \frac{\lambda_{\text{th}}}{V}.$$

Therefore the 1σ uncertainty in λ_{th} induced by an uncertainty ΔV in the accelerating voltage is

$$\sigma_{\lambda_{\text{th}}} = \left| \frac{\partial \lambda_{\text{th}}}{\partial V} \right| \Delta V = \frac{1}{2} \lambda_{\text{th}} \frac{\Delta V}{V}. \quad (7)$$

If the voltage uncertainty is given as a fractional uncertainty $\delta_V = \Delta V/V$ (e.g. $\delta_V = 0.01$ for 1% uncertainty), then $\sigma_{\lambda_{\text{th}}} = \frac{1}{2} \delta_V \lambda_{\text{th}}$.

We see that our calculations match within $1 - \sigma$

7 Limitations and Sources of Error

Several factors limit the accuracy and precision of the electron diffraction experiment:

Measurement of ring diameters

The dominant source of experimental uncertainty arises from measuring the diffraction ring diameters on the curved fluorescent screen:

- The rings are not infinitely sharp but have a finite thickness, making it difficult to define the exact diameter.
- Parallax errors occur if the observer is not aligned perpendicularly to the screen during measurement.
- Vernier calipers typically provide a resolution of about ± 0.5 mm, which propagates directly into uncertainties in the calculated wavelengths.

Geometrical approximations

The relationship between the ring diameter D , the distance to the screen L , and the diffraction angle θ is often approximated as $\sin \theta \approx D/(2L)$. This small-angle approximation introduces systematic error, particularly for larger diameters where curvature effects of the screen are non-negligible. A more accurate relation includes the radius of curvature R of the spherical screen.

Voltage stability and calibration

The theoretical de Broglie wavelength depends on the accelerating voltage V as $\lambda \propto 1/\sqrt{V}$. Even small fractional uncertainties in V propagate into the calculated wavelength. Additional error may arise from:

- Power supply fluctuations and voltage drift during the measurement.
- Limited resolution of the voltmeter or digital display on the high-voltage source.
- Contact resistance and imperfect connections in the circuit.

Graphite target

The target foil is polycrystalline graphite, consisting of many small crystallites with random orientations. Although this ensures the appearance of diffraction rings, the effective lattice spacing d used in Bragg's law is taken from literature values. Variations in foil quality, thickness, or crystal defects may shift the effective interplanar spacing and broaden the rings.

Other experimental limitations

- Alignment of the electron beam and focusing voltages affect the clarity of the rings. Misalignment can distort the ring geometry.
- The fluorescent screen may degrade with prolonged exposure, reducing contrast and making precise measurement more difficult.
- Mechanical vibrations or accidental movement of the apparatus during data collection can slightly alter ring positions.

8 Conclusions and Discussion

Discussion of results

The experiment successfully demonstrated the wave nature of electrons by producing clear diffraction rings when an electron beam was incident on a polycrystalline graphite target. By measuring the diameters of the inner and outer rings and applying Bragg's law, the wavelengths of the electrons were calculated for different accelerating voltages.

The experimentally determined wavelengths, both from the (100) and (110) lattice planes of graphite, were found to be in reasonable agreement with the theoretical de Broglie wavelengths,

$$\lambda = \frac{h}{\sqrt{2m_e eV}}.$$

This confirms de Broglie's hypothesis that matter exhibits wave-like properties, with the electron behaving as both a particle and a wave.

Although the data generally followed the expected trend of decreasing wavelength with increasing voltage, small discrepancies were observed. The deviations between measured and theoretical values were typically within the propagated 1σ uncertainties. In some cases, systematic shifts were evident, likely due to geometric approximations, measurement challenges, or voltage calibration issues.

Conclusions

- The diffraction of electrons by graphite was clearly observed, producing concentric diffraction rings consistent with Bragg reflection from lattice planes.
- The measured wavelengths from both (100) and (110) reflections decreased with increasing accelerating voltage, in accordance with de Broglie's prediction.
- Quantitative comparison showed that the experimental results agree with the theoretical de Broglie wavelengths within experimental uncertainties, providing strong evidence for electron wave-particle duality.

Broader implications

This experiment mirrors the pioneering Davisson–Germer experiment and provides a direct laboratory verification of quantum mechanics. It highlights how diffraction and interference, phenomena usually associated with light, also arise in the behavior of matter particles. Beyond verifying the de Broglie relation, the method illustrates the use of scattering experiments to probe atomic structure—a principle central to modern particle and condensed matter physics.

Outlook

Future improvements, such as digital imaging of diffraction patterns, automated diameter measurement, and more precise voltage control, would reduce uncertainties and minimize systematic errors. Such refinements could enable extraction of Planck's constant from the data with greater accuracy, extending the educational value of the experiment.

References

- [1] Fujiwara, *Relativistic Dynamical Theory of Electron Diffraction*, Journal of the Physical Society of Japan, Vol II, 1961
- [2] Ashcroft & Mermin, *Solid State Physics*, Second Edition
- [3] Hirsch, Howie, et al., *Electron Microscopy of Thin Crystals*
- [4] Cowley, *Diffraction Physics*, North-Holland Personal Library, 1995
- [5] IISER Pune Physics Lab 5 Manual

Appendix

Collected Raw Data

Electron Diffraction		
V (in KV)	d2 (smaller radius) (mm)	d1 (larger radius) (mm)
2	34.84	54.362
2.5	28.88	43.348
3	26.66	45.00
3.5	24.62	42.34
4	22.88	40.02 38.88888888888888
4.5	21.68	37.22 38.88888888888888
5	20.86	55.328

Tanay
20/8/25